

# Changes in Effective Connectivity of the Superior Parietal Lobe during Inhibition and Redirection of Eye Movements

## Supplementary Issue: Behavioral Neuroscience

Susanne J. Asscheman<sup>1</sup>, Katharine N. Thakkar<sup>1,2</sup> and Sebastiaan F.W. Neggers<sup>1</sup>

<sup>1</sup>Department of Psychiatry, Brain Center Rudolf Magnus, University Medical Center Utrecht, Utrecht, The Netherlands.

<sup>2</sup>Department of Psychology, Michigan State University, East Lansing, MI, USA.

**ABSTRACT:** Executive control is the ability to flexibly control behavior and is frequently studied with saccadic eye movements. Contrary to frontal oculomotor areas, the role of the superior parietal lobe (SPL) in the executive control of saccades remains unknown. To explore the role of SPL networks in saccade control, we performed a saccadic search-step task while acquiring functional magnetic resonance imaging data for 41 participants. Psychophysiological interaction analyses assessed task-related differences in the effective connectivity of SPL with other brain regions during the inhibition and redirection of saccades. Results indicate an increased coupling of SPL with frontal, posterior, and striatal oculomotor areas for redirected saccades versus visually guided saccades. Saccade inhibition versus unsuccessful inhibition revealed an increased coupling of SPL with dorsolateral prefrontal cortex and anterior cingulate cortex. We discuss how these findings relate to ongoing debates about the implementation of executive control and conclude that early attentional control and rapid updating of saccade goals are important signals for executive control.

**KEYWORDS:** executive control, saccades, effective connectivity, search-step task, superior parietal lobe

**SUPPLEMENT:** Behavioral Neuroscience

**CITATION:** Asscheman et al. Changes in Effective Connectivity of the Superior Parietal Lobe during Inhibition and Redirection of Eye Movements. *Journal of Experimental Neuroscience* 2015:9(S1) 27–40 doi:10.4137/JEN.S32736.

**TYPE:** Original Research

**RECEIVED:** October 8, 2015. **RESUBMITTED:** February 11, 2016. **ACCEPTED FOR PUBLICATION:** February 19, 2016.

**ACADEMIC EDITOR:** Lora Watts, Editor in Chief

**PEER REVIEW:** Three peer reviewers contributed to the peer review report. Reviewers' reports totaled 2206 words, excluding any confidential comments to the academic editor.

**FUNDING:** This work was supported by a Netherlands Organization for Scientific Research Rubicon Grant (KNT), Utrecht University (Short-Stay Fellowship to KNT and a Neuroscience and Cognition Grant to SFWN). The authors confirm that the funder had no influence over the study design, content of the article, or selection of this journal.

**COMPETING INTERESTS:** Authors disclose no potential conflicts of interest.

**COPYRIGHT:** © the authors, publisher and licensee Libertas Academica Limited. This is an open-access article distributed under the terms of the Creative Commons CC-BY-NC 3.0 License.

**CORRESPONDENCE:** susanneasscheman@hotmail.com

Paper subject to independent expert single-blind peer review. All editorial decisions made by independent academic editor. Upon submission manuscript was subject to anti-plagiarism scanning. Prior to publication all authors have given signed confirmation of agreement to article publication and compliance with all applicable ethical and legal requirements, including the accuracy of author and contributor information, disclosure of competing interests and funding sources, compliance with ethical requirements relating to human and animal study participants, and compliance with any copyright requirements of third parties. This journal is a member of the Committee on Publication Ethics (COPE).

Published by Libertas Academica. Learn more about this journal.

## Introduction

Executive control is the ability to flexibly control behavior on the basis of current task demands. One important aspect of executive control is the ability to rapidly inhibit or change prepared action plans, if these responses become inappropriate—a function referred to as reactive control.<sup>1</sup>

The saccadic eye movement system is an ideal effector system for investigating the executive control of action, as the neural circuitry of saccade initiation has been well described in nonhuman primates.<sup>2–7</sup> Tasks such as the countermanding paradigm task and search-step task have been used to specifically probe reactive executive control of saccades.<sup>8–11</sup> Both tasks require rapid saccades to a target, and occasionally, the planned saccade can be inhibited or redirected upon the sudden presentation of a visual or auditory stimulus (stop or change signal).

Neurophysiology studies have highlighted a network of regions involved in saccade initiation. The key regions in this network include frontal eye fields (FEF) and intraparietal sulcus that project to subcortical areas, such as the striatum and superior colliculus (SC), pivotal for preparation and generation of saccades.<sup>7</sup> During saccade initiation, FEF

neurons discharge until a threshold is reached, upon which a saccade is executed.<sup>12,13</sup> Importantly, in macaques performing the countermanding task, neuronal firing in the FEF is attenuated following a stop signal on trials in which the animal successfully inhibited a saccade.<sup>14,15</sup> It has been suggested that modulation of FEF neurons to either execute or inhibit a saccade is implemented by the supplementary eye fields (SEF) and the dorsolateral prefrontal cortex (DLPFC).<sup>3,8</sup> However, during countermanding task performance, SEF neurons modulate too late after a stop signal to be directly involved in saccade control; instead, data suggest that the SEF and nearby anterior cingulate cortex (ACC) play a larger role in monitoring the response outcomes and biasing behavior over a longer time scale.<sup>16–21</sup> DLPFC neurons on the other hand can influence the excitability of the oculomotor system on a rapid time scale.<sup>3</sup> That is, task cues and stimulus location are integrated by DLPFC neurons to either execute or inhibit a planned saccade, depending on current task demands.<sup>22</sup>

Along with cortical regions, subcortical structures also contribute to rapid control over eye movements. The basal ganglia exert their control by either inhibiting or disinhibiting



a saccade through the direct and indirect pathways, respectively, depending on the behavioral demands.<sup>6</sup> Subsequently, the basal ganglia output their signals to the SC, which plays a key role in orienting and saccadic control and directly controls the oculomotor neurons in the pons that drive the eye muscles.<sup>23</sup>

Contrary to frontal cortex and subcortical structures,<sup>24–26</sup> the role of the parietal cortex during rapid control of saccades has received less attention. Of particular interest is the superior parietal lobe (SPL). The SPL is a part of the dorsal–dorsal stream consisting of area V6, parieto-occipital cortex, and the SPL.<sup>27</sup> The SPL is considered to be the human homolog of the monkey lateral intraparietal area (LIP).<sup>28,29</sup> Single-cell recordings from LIP neurons showed that activity of these neurons was related to the locus of attention.<sup>30</sup> Moreover, activity in these neurons was associated with the probability that a target was the endpoint of the next saccade. This suggests that LIP is an important area in the attentional control of saccades. However, other studies suggest that LIP neurons code target location for action planning in an eye-centered reference frame.<sup>31–33</sup> This reference frame encoding of target location was also found in human parietal cortex.<sup>34</sup> This is also a relevant capacity during rapid control of saccades to changing target locations, as the desired endpoint needs to be encoded in a spatial reference frame allowing fast saccadic reprogramming and associated spatial updating across saccades.

Functional imaging studies of the SPL in humans are consistent with neurophysiology studies and underscore its role in the attentional guidance of saccades. Spatial attention shifts were related to increased activity in the SPL.<sup>35</sup> In addition, changes in target and/or distractor location are coded by the SPL. These changes are applied to the attentional priority map that is created by the intraparietal sulcus.<sup>35–38</sup> This attentional priority map enables us to attend to salient stimuli and ignore distractors. The role of the SPL in the top-down control of attention is further supported by lesion and transcranial magnetic stimulation studies.<sup>39–41</sup> Together, these studies suggest a role of the SPL in the attentional guidance of saccadic eye movements; however, its involvement in rapid control over movement initiation (eg, inhibition and redirection) is less clear.

Several functional imaging studies of the parietal cortex showed increased activity on trials in which executive control over saccades is required compared to simple visually guided saccades.<sup>42,43</sup> However, additional research is necessary to obtain a more complete understanding of its exact function. The goal of this study was to examine the role of SPL during rapid inhibition and redirection of eye movements. We were specifically interested in the changes in the effective connectivity between the SPL and other oculomotor areas during the higher order control of saccadic eye movements.

This study is relevant since the role of SPL in the ability to rapidly control behavior, potentially via early attentional

processes or changes in reference frame encoding, remains largely unknown. Previous studies have shown that early perceptual processing of a target can significantly influence the efficiency of executive control over saccadic eye movements and, therefore, is an important aspect of performance on the countermanding and double-step tasks.<sup>44,45</sup> This study addresses this topic and asks whether successful inhibition and redirection is related to increased coupling between early attentional areas and other areas of the oculomotor system. By examining the effective connectivity of the SPL during rapid control of saccadic eye movements, we might provide new evidence regarding the SPL as an important area in the neural circuitry underlying the executive control of saccades in humans, and perhaps in association the role of attentional processing. Previous research typically focused on the frontal cortical and basal ganglia areas and their role in rapid control of saccades. To our knowledge, this is the first study using an SPL seed region during effective connectivity analysis to unravel the role of the SPL in saccadic control.

Saccadic eye movements were assessed using the saccadic search-step task as described in a previous publication.<sup>26</sup> Forty-one healthy subjects performed this task during functional magnetic resonance imaging (fMRI). Bilateral SPL was taken as seed region during psychophysiological interaction (PPI) analysis. With PPI, we are able to infer the task-related differences in the connectivity of the SPL both between trials in which rapid executive control of saccades is required and not required and between trials in which the inhibition is successful and not successful. This study has the potential to shed light on the role of the SPL in the rapid control of saccadic eye movements.

## Methods

**Participants.** Forty-two healthy volunteers participated in this study. Due to excessive head motion in the scanner, one participant was excluded, leaving 41 participants (20 males, mean age 29.8 years) for further analyses. Thirty-three participants were right handed, five participants were left handed, and three participants were ambidextrous as was assessed with the Edinburgh Handedness Inventory. Participants had normal vision or corrected to normal vision. Exclusion criteria were a history of neurological or psychiatric disorders or a history of traumatic brain injury. Participants provided an informed written consent before participation and received monetary compensation for their time. All procedures were approved by the ethics committee of the University Medical Center Utrecht. The research was conducted in accordance with the principles of the Declaration of Helsinki.

**Saccadic search-step task.** The saccadic search-step task (Fig. 1), also described in a previous publication with a subset of the participant,<sup>26</sup> consisted of three different types of trials: no-step trials (30%), follow trials (30%), and redirect trials (40%). The trial duration was four seconds. Trials were presented after an intertrial interval of 1000–2000 ms. At the

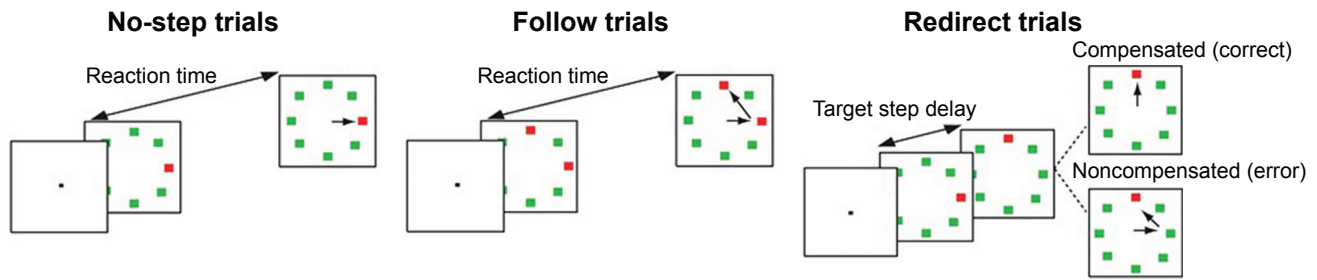


**Figure 1.** The saccadic search-step task. A trial started after an intertrial interval of 1000–2000 ms. At the start of each trial, an eight-element array was presented. On no-step trials, a red target was presented among seven green distractors. Participants were instructed to make a saccade to the red target. On follow trials, an array was presented with two red targets, and participants were instructed to make a saccade to both target locations, one after the other. On redirect trials, the first target location (T1) became a distractor, and a new target location (T2) appeared after a certain TSD after initial array presentation. Participants were instructed to inhibit the first planned saccade to T1 and directly make a saccade to T2. Trials in which participants correctly inhibited the planned saccade to T1 and made a saccade directly to T2 were labeled as compensated trials. Trials in which participants failed to inhibit the planned saccade and, thus, first made a saccade to T1 and subsequently to T2 are labeled as noncompensated. TSD was adjusted online using a tracking procedure to ensure ~50% success rate on redirect trials. Image is from our previous publication.<sup>26</sup>

start of each no-step trial and redirect trial, an eight-element array was presented containing one red target among green distractors. The isoluminant elements subtended  $0.7^\circ$  visual angle and were presented  $9^\circ$  of visual angle from the center of the array. On no-step trials, the target location remained the same. However, on redirect trials, there was an isoluminant color change of the first red target (T1) into a green distractor at a delay after initial array presentation (target step delay [TSD]) and a new red target appeared at a new target location (T2). On no-step trials, a single saccade to the presented red target was required. However, on redirect trials, participants were instructed to inhibit the initial planned saccade to the first location (T1) and redirect their gaze toward the new cued location (T2). Trials in which participants successfully inhibited a saccade to T1 and made a direct saccade to T2 were labeled as compensated trials. Trials in which participants failed to inhibit the initial planned saccade to T1 were labeled as noncompensated trials. These erroneous saccades are often followed by a corrective saccade to T2.<sup>46</sup> On follow trials, two red targets among green distractors were presented on the eight-elementary array. Participants were instructed to make saccades to both T1 and T2, one after the other. The order in which participants attended the targets during follow trials was irrelevant. Follow trials were included to match the number of saccades on noncompensated trials. As a result, we could examine the activation related to error processing by setting up a contrast for noncompensated trials versus follow trials as was done for the previous study on this data.<sup>26</sup> On both redirect trials and follow trials, T1 and T2 were separated from each other with a minimum polar angle of  $90^\circ$  to diminish the possibility of a saccade landing mid-way between T1 and T2.<sup>47</sup>

With longer TSDs, it becomes increasingly difficult to inhibit.<sup>9</sup> Therefore, the accuracy of redirect trials was manipulated by using a one-up/one-down tracking procedure, ensuring successful inhibition in ~50% of the redirect trials.

TSD started at 100 ms and was increased or decreased by 67 ms following the compensated or noncompensated trials, respectively. In total, four runs were executed with 60 trials per run (72 no-step trials, 72 follow trials, and 96 redirect trials). The three types of trials were interleaved, and participants were not explicitly instructed about the relative frequency of the different trial types. Six null trials per run were added as baseline during which the participants fixated on a cross for 10 seconds.

Participants were instructed and trained on the saccadic search-step task prior to the MRI session. During the instructions, it was stressed that both speed and accuracy were important. In addition, participants were informed that on redirect trials, inhibiting the saccade to T1 would not always be possible.

**Stimulus display and eye tracking.** Stimuli were presented on an magnetic resonance (MR)-compatible light emitting diode (LED) screen using the Presentation software (Neurobehavioral Systems). The screen was placed at the end of the bore of the MR scanner and could be watched by the participants via a mirror that was attached to the head coil. An MR-compatible infrared eye tracker mounted to the head coil was used to record eye movements online during the scanning session. LED lights on the head coil provided infrared illumination. Eye position was sampled at a rate of 60 Hz and was acquired using the ViewPoint eye tracking software (Arrington Research). To calculate the accurate timing of saccades, presented stimuli were encrypted digitally, forwarded to the ViewPoint software, and inserted as triggers in the eye movement recordings.

Accuracy on redirect trials was measured online to adjust TSD. Therefore, information about eye position on each trial was stored in a memory buffer. Eye position was drift corrected after redirect trials. This was done by using the mean eye position in a 50 ms time window around array presentation. The accuracy on these redirect trials was then



determined using a position criterion. Trials were considered as compensated trials if the eye moved outside a window spanning  $2^\circ$  of visual angle around fixation after 100 ms following array presentation for at least two samples (33 ms) and was directed toward T2. Next, the TSD was increased for the following redirect trial. Redirect trials in which the eye moved toward T1 were labeled as noncompensated, and TSD for the next trial decreased. On trials in which the eye position was neither in the direction of T1 nor in the direction of T2, perhaps due to eye tracker noise or blinking, TSD was maintained.

**Scoring and analysis of eye movement.** Eye movement data were analyzed offline in MATLAB (The MathWorks). Eye velocity was obtained by differentiating the eye position data and filtered using a fifth-order Butterworth filter with a cutoff of 40 Hz. A liberal velocity criterion was used to automatically establish saccade onset. Invalidly marked saccades (eg, camera noise/blinks) were manually removed. Saccades with an onset of less than 100 ms after array onset were excluded from further analysis. Directional accuracy was automatically scored. Saccade latency was defined as the time between the onset of a saccade and the array onset. For compensated trials, the time between the onset of T2 and the onset of the saccade was used as saccade latency.

**Image acquisition.** Scans were acquired using a 3.0 T Achieva MRI scanner (Philips Medical Systems) located at the University Medical Center Utrecht. Parallel imaging was achieved by sensitive encoding (SENSE) with an eight-channel head coil. Whole-brain T2\*-weighted echo planar imaging was acquired for blood-oxygen level-dependent (BOLD) contrast (repetition time [TR] = two seconds, echo time [TE] = 35 ms, field of view = 256 mm  $\times$  256 mm  $\times$  120 mm, matrix = 96  $\times$  96  $\times$  35, voxel size = 2.67 mm  $\times$  2.67 mm  $\times$  3.42 mm, and flip angle =  $70^\circ$ ). For each of the four sessions, 152 volumes were acquired with 35 slices per volume. Slices were acquired interleaved in the transverse plane. To allow for T1 equilibrium saturation effects, the first six volumes of each run were discarded. For within-subject registration, whole-brain three-dimensional fast field echo T1-weighted images were acquired (200 slices, TR = 10 ms, TE = 4.6 ms, field of view = 240 mm  $\times$  240 mm  $\times$  160 mm, voxel size = 0.75 mm  $\times$  0.8 mm  $\times$  0.75 mm, and flip angle =  $8^\circ$ ). Cardiac and respiratory pulsatility measures were used to correct for nonneural effects. Cardiac signals were acquired at 500 Hz with electrocardiogram (ECG) electrodes. Respiratory measures were recorded at 500 Hz with a wrap band around the midsection.

#### Data analysis.

**Preprocessing.** Functional images were preprocessed and analyzed using Statistical Parametric Mapping version 8 (SPM8) (<http://www.fil.ion.ucl.ac.uk/spm/software/spm8>) and MATLAB. Initially, functional images were realigned using the six rigid body transformations to correct for head motion. A mean functional image was created for each subject. To correct for timing differences in slice acquisition, slice time

correction was performed. Slice time acquisition was temporally interpolated over each slice to match to the acquisition time of the middle slice. The anatomical image of each subject was aligned to its mean functional image with a normalized mutual information criteria method. The anatomical image was further segmented and normalized into Montreal Neurological Institute (MNI) space using a unified segmentation method.<sup>48</sup> These normalization parameters were applied to the functional images. Finally, a Gaussian kernel of 6 mm full width half maximum was used to spatially smooth the functional images.

**General linear model analysis.** A first-level general linear model (GLM) was performed. The design matrix included no-step, follow-up, compensated, and noncompensated trials as the regressors of interest. No-step reaction times were split into fast and slow trials based on the percentile corresponding to the proportion of noncompensated trials. Latency matching is frequently done in neurophysiology and electrophysiology countermanding studies and might result in a more sensitive model of neural activation.<sup>10,15</sup> Latency matching is best described by the horse-race model logic.<sup>49,50</sup> The horse-race model states that go stimuli and stop stimuli can trigger a GO process and STOP process, respectively. These two processes race against each other toward a threshold. The finishing time of both processes determines the behavioral outcome. That is, if the GO process finishes before the STOP process, an action is initiated, whereas if the STOP process reaches the threshold first, an action is inhibited. On compensated trials, the GO process has not progressed far enough and is still susceptible for inhibition by the STOP signal. The GO latency of these compensated trials matches with that of no-step slow trials, based on the model discussed earlier.<sup>26</sup> This means that if a target step would have occurred during these no-step slow trials, inhibition would still have been possible. Therefore, no-step trials were split into fast and slow trials to match the latencies of noncompensated and compensated trials, respectively. No-step fast and no-step slow trials were entered into the design matrix as independent regressors of interest. Fixation trials were used as an implicit baseline and, therefore, are not modeled. The regressors were constructed using delta functions coding for array onset over time per factor and were then convolved using a canonical hemodynamic response function as implemented in the Statistical Parametric Mapping version 8. Twenty nuisance regressors were added to model nonneural signals (eg, respiratory and pulsatility effects) using the RETROICOR method with fifth-order Fourier expansion.<sup>51</sup>

A white matter regressor, reflecting the signal over time in the white matter, was added to remove any additional movement-related activity in the neural signal.<sup>52,53</sup> The white matter regressor was constructed by taking the average first eigenvariate of the time series of two white matter voxels in the posterior corona radiata (MNI coordinates: left [-28 -41 22] and right [30 -41 22]). Accordingly, the white matter regressor reflects a pure white matter signal because



of its location in this white matter tract. Finally, three block regressors and the intercept were added to the model as well. Data were also prewhitened to remove any temporal autocorrelation in the data by using a first order autoregressive model. Data were high-pass filtered during prewhitening at a frequency of 70 Hz.

Contrast images were generated for compensated trials versus no-step slow trials to examine the activation related to the inhibition and redirection of eye movements. On both trial types, participants generate one task-related saccade per trial. However, on compensated trials, participants have to inhibit and redirect their saccade. The difference between the two trial types reflects a process of inhibition and redirection and is illustrated by activation differences in this contrast. To examine the activation related to successful inhibition versus unsuccessful inhibition, a contrast image was created to compare compensated trials with noncompensated trials. The difference between these trial types mainly is the failure to inhibit the first planned saccade on noncompensated trials. Therefore, activation in this contrast reflects the process of successful inhibition. When interpreting the results of this later contrast, one should take into account putative differences in activation since the number of saccades does not match in the two conditions. Namely, on compensated trials, only one saccade is produced, while on noncompensated trials, two saccades are typically produced (erroneous and corrective saccade).

Individual contrast images were submitted to a second-level random-effects analysis to test for whole-brain within group effects using one-sample  $t$  tests. Statistical inferences were made at a voxel threshold of  $P < 0.05$  with family-wise error (FWE) correction using Gaussian random fields to account for multiple comparisons.<sup>54,55</sup>

**PPI analysis.** A PPI analysis was conducted according to the procedure described by Friston et al.<sup>56</sup> With PPI, condition-specific changes in effective connectivity are assessed between a seed region and the rest of the brain.

To study the differences in the effective connectivity during rapid control of saccades, two contrasts of interest were set up. The first contrast was set up to compare the differences in effective connectivity during compensated trials versus no-step slow trials. The difference between the two conditions reflects changes in effective connectivity during an inhibitory process to T1 and a redirection process to T2. The second contrast was set up to compare the differences in effective connectivity during compensated trials versus noncompensated trials. The difference reflects changes in effective connectivity during a successful inhibitory process to T1 compared to an unsuccessful inhibitory process to T1.

A significant PPI indicates a difference in connectivity with the seed region during one task condition versus another task condition. This PPI result can be either positive or negative, suggesting an increase or a decrease in connectivity, respectively. Seeds were selected based on the local maximum of a

significant cluster in the basic GLM analysis testing the contrast compensated trials versus no-step slow trials. In addition, the seed was anatomically restricted to the SPL according to the Automated Anatomical Labeling atlas.<sup>57</sup> Based on these criteria, time series were extracted from two 6 mm seeds, one placed in left SPL (MNI coordinates:  $-18 -63 54$ ) and one in right SPL (MNI coordinates:  $27 -63 51$ ).

The first eigenvariate of the time series in the seed region was multiplied by the psychological vector to create the PPI term. This interaction term was orthogonalized with respect to the seed time series and psychological condition to estimate the effect of the interaction term without influences of the main effect of time series and psychological regressor. The design matrix for the PPI GLM included the interaction term, the first eigenvariate of the seed time series, a psychological condition vector, 20 nuisance regressors, three block regressors coding session baseline, one white motion regressor, and the intercept. Regressors were constructed as described earlier.

The first-level contrast images were entered into a second-level random-effects analysis to test for whole-brain within group effects using one-sample  $t$  tests. Statistical inferences were made at a cluster threshold of  $P < 0.05$  with FWE correction using Gaussian random fields to account for multiple comparisons.<sup>54,55</sup>

## Results

**Behavior.** The behavioral results for the entire group of participants can be found in our previous publication by Thakkar et al.<sup>26</sup>

### GLM analysis.

*Compensated trials versus no-step slow trials.* To examine the activity related to the inhibition and redirection of the saccade plan, compensated trials were contrasted with no-step slow trials. There was an increased activation frontally in bilateral SEF, FEF, and right inferior frontal cortex (IFC) for compensated trials compared to no-step slow trials (Fig. 2). Increased parietal activation was found bilaterally in the SPL and inferior parietal lobe (IPL). Bilateral fusiform gyrus, right middle temporal cortex, and bilateral visual cortex also showed an increased activation during compensated trials as opposed to no-step slow trials. There were no regions of decreased activation for this contrast. These results parallel our published findings using a subset of these participants.<sup>26</sup>

*Compensated trials versus noncompensated trials.* Compensated trials were contrasted with noncompensated trials to study the activity related to successful inhibition versus unsuccessful inhibition. This analysis did not yield any significant increased or decreased activation for compensated trials compared to noncompensated trials even at FWE-corrected  $P < 0.1$ . Again, these findings replicate the results found in our previous study.<sup>26</sup>

### PPI analyses.

*Compensated trials versus no-step slow trials.* To examine the changes in the effective connectivity of the SPL with

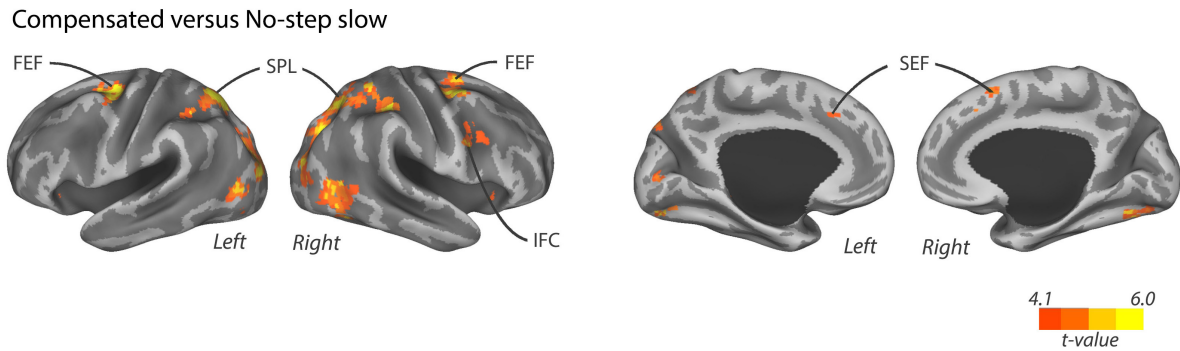


**Figure 2.** BOLD activation for regions that showed increased activity for compensated trials compared to no-step slow trials. Activation is shown at an uncorrected threshold of  $P < 0.0001$ .

other brain regions during the inhibition and redirection of saccades, PPI analyses were performed for compensated trials versus no-step slow trials using bilateral SPL as seed regions.

Results of this PPI contrast showed that right SPL coupled more strongly with bilateral SEF and right FEF for compensated trials versus no-step slow trials. Moreover, several posterior cortical areas also showed an increased coupling with the right SPL, including right supramarginal gyrus (SMG), right precuneus, bilateral IPL, and left visual cortex during compensated trials versus no-step slow trials (Table 1 and Fig. 3A). Subcortically, we found an increased coupling of right SPL with the left putamen for compensated trials compared to no-step slow trials. The positive PPI plots for left SEF, right SMG, bilateral IPL, and left visual cortex when right SPL was taken as seed in a representative individual are shown in Figure 4. The dots in Figures 4–6 are residual fMRI time series data (activation factored out) for every single time point acquired in succession. This is the

signal the PPI measures (steepness of slope) are based on. This is a common distribution to plot in PPI analysis<sup>56</sup> to provide further insight in the single scan data the analysis is based on.

PPI analysis for compensated trials versus no-step slow trials using left SPL as seed revealed a similar effective connectivity network in the right hemisphere. For example, left SPL also showed an increased coupling with the frontal oculomotor regions, the right SEF and right FEF, for compensated trials. In the parietal cortex, we again found a stronger coupling with the right SMG. Moreover, left SPL showed an increased coupling with right SPL for compensated trials. Furthermore, occipital areas along the dorsal visual processing stream showed an increased coupling with the left SPL, namely left parieto-occipital cortex and bilateral visual cortex, during compensated trials compared to no-step slow trials. Finally, increased coupling was found between left SPL and right fusiform gyrus during compensated trials (Fig. 3B and Table 1).

**Table 1.** Local maxima of PPI analysis for compensated trials versus no-step slow trials and compensated trials versus noncompensated trials.

SEED REGION	CLUSTER SIZE	CLUSTER CORRECTED P	T STATISTICS	Z STATISTICS	CLUSTER COORDINATES			MNI REGION
					X	Y	Z	
Right SPL Compensated versus no-step slow	120	0.001	5.74	4.88	57	-36	33	Right supramarginal
			3.98	3.63	60	-21	45	Right postcentral
			3.95	3.61	60	-15	36	Right postcentral
	244	0	5.39	4.65	-6	6	51	Left SMA (SEF)
			4.23	3.82	12	9	69	Right SMA (SEF)
			3.96	3.62	6	0	69	Right SMA (SEF)
	68	0.014	4.65	4.13	18	-72	42	Right precuneus
	84	0.005	4.55	4.06	33	-51	54	Right inferior parietal
			4.51	4.03	33	-45	39	Right inferior parietal
	193	0	4.50	4.02	-33	-54	48	Left inferior parietal
			4.42	3.96	-39	-36	39	Left inferior parietal
			4.35	3.91	-45	-39	48	Left inferior parietal

(Continued)



Table 1. (Continued)

SEED REGION	CLUSTER SIZE	CLUSTER CORRECTED P	T STATISTICS	Z STATISTICS	CLUSTER COORDINATES			MNI REGION
					X	Y	Z	
Left SPL	76	0.008	4.47	4.00	-21	9	3	Left putamen
			4.09	3.71	-12	3	-3	Left pallidum
	65	0.018	4.14	3.75	33	-3	45	Right SMA
			3.81	3.50	30	0	57	Right SMA
	145	0	3.74	3.44	45	-3	48	Right SMA (FEF)
			4.07	3.70	-24	-87	12	Left middle occipital
	470	0	4.00	3.65	0	-78	3	Left lingual
			4.00	3.65	0	-93	6	Left calcarine
	186	0	5.75	4.88	12	9	66	Right SMA (SEF)
			5.64	4.81	-6	9	42	Left middle cingulum
	138	0	4.86	4.28	9	0	66	Right SMA (SEF)
			5.22	4.53	54	-36	30	Right supramarginal
	96	0.002	4.64	4.12	48	-42	27	Right supramarginal
			5.18	4.50	0	-78	-3	Left lingual
	99	0.002	4.30	3.88	6	-84	6	Right calcarine
			3.82	3.51	-6	-75	-12	Left cerebellum
	55	0.033	4.91	4.32	-30	-60	-21	Left cerebellum
			4.52	4.04	-18	-78	-6	Left lingual
	113	0.001	4.24	3.83	-21	-66	-18	Left cerebellum
			4.67	4.15	18	-72	45	Right precuneus
90	0.003	4.04	3.68	6	-63	51	Right precuneus	
		3.86	3.54	15	-60	54	Right superior parietal	
66	0.015	4.53	4.05	-36	18	0	Left insula	
		3.88	3.55	-45	6	3	Left insula	
71	0.025	4.48	4.01	45	9	3	Right insula	
		4.33	3.90	36	15	3	Right insula	
58	0.027	3.90	3.57	48	12	-6	Right insula	
		4.43	3.98	-21	-66	33	Left superior occipital	
66	0.015	4.41	3.96	-33	-51	45	Left inferior parietal	
		3.69	3.40	-9	-66	42	Left precuneus	
119	0.002	4.31	3.88	27	-6	45	Right middle frontal (FEF)	
		3.81	3.50	33	9	63	Right middle frontal (FEF)	
71	0.025	3.77	3.47	27	9	54	Right middle frontal (FEF)	
		4.03	3.67	36	-66	-15	Right fusiform	
71	0.025	3.76	3.46	27	-57	-15	Right fusiform	
		4.49	4.02	6	27	42	Right dorsal ACC	
71	0.025	3.85	3.53	-3	6	42	Left ventral ACC	
		3.77	3.47	-12	3	54	Left SMA (SEF)	
71	0.025	4.18	3.78	-24	39	42	Left superior frontal (DLPFC)	
		4.07	3.70	-24	51	18	Left middle frontal (DLPFC)	
71	0.025	3.69	3.40	-24	39	27	Left middle frontal (DLPFC)	

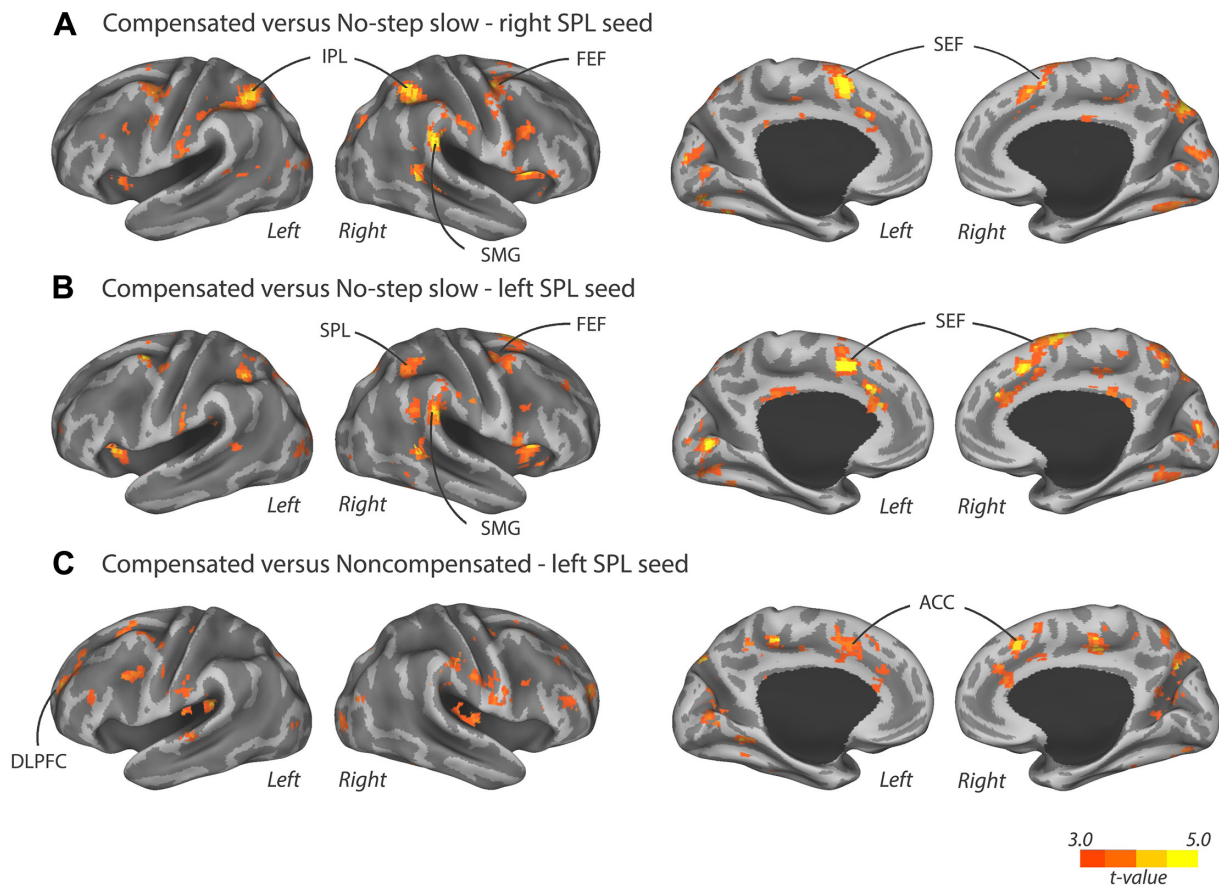


**Figure 3.** Regions where the PPI term was greater for compensated trials than no-step slow trials when (A) right SPL was chosen as seed region or (B) left SPL was chosen as seed region. (C) Regions where the PPI term was greater for compensated trials than noncompensated trials when left SPL was chosen as seed region. Significant clusters after FWE correction are displayed on an inflated surface and are displayed in Table 1. Activation is presented at an uncorrected threshold of  $P < 0.001$ .

Positive PPI plots for right SEF, right FEF, right SMG, and left visual cortex when left SPL was taken as a seed in a representative individual are shown in Figure 5.

There was no evidence of decreased coupling between left or right SPL and other brain regions for this contrast (decreased PPI coupling is by itself equally informative and physiologically meaningful as increased coupling).

*Compensated trials versus noncompensated trials.* To examine the effective connectivity network involved in successful inhibition versus unsuccessful inhibition, we performed a PPI analysis investigating the effective connectivity of bilateral SPL during compensated versus noncompensated trials. Analyses using the left SPL as a seed region showed a significantly increased coupling with bilateral ACC and left DLPFC (Fig. 3C) during compensated trials compared to noncompensated trials. The positive PPI plots for right ACC and left DLPFC in a representative individual are shown in Figure 6. The right SPL seed failed to show significant coupling with any brain region. Moreover, we did not find any decreased coupling between right or left SPL and other regions for compensated trials compared to noncompensated trials.

## Discussion

The aim of this study was to examine the effective connectivity between the superior parietal cortex and other brain regions during rapid executive control of eye movements. We compared the connectivity between trials in which executive control is required and not required (ie, compensated trials versus no-step slow trials) and trials in which inhibition is successful and not successful (ie, compensated trials versus noncompensated trials). We proposed that the SPL could contribute significantly to rapid control of eye movements, potentially via early attentional control or rapid updating of saccade goal.

The results of the basic GLM reveal an increased activation in several oculomotor areas for compensated trials compared to latency-matched no-step trials. For example, the observed activation in the FEF during compensated trials might reflect an inhibitory process during compensated trials to T1 as FEF neurons have been shown to modulate during the cancellation of a saccade.<sup>15</sup> Similarly, the detected activation in IPL is consistent with a previous countermanding study and also seem to reflect an inhibition process.<sup>58</sup> Greater activation in the SEF might be related to increased sensitivity



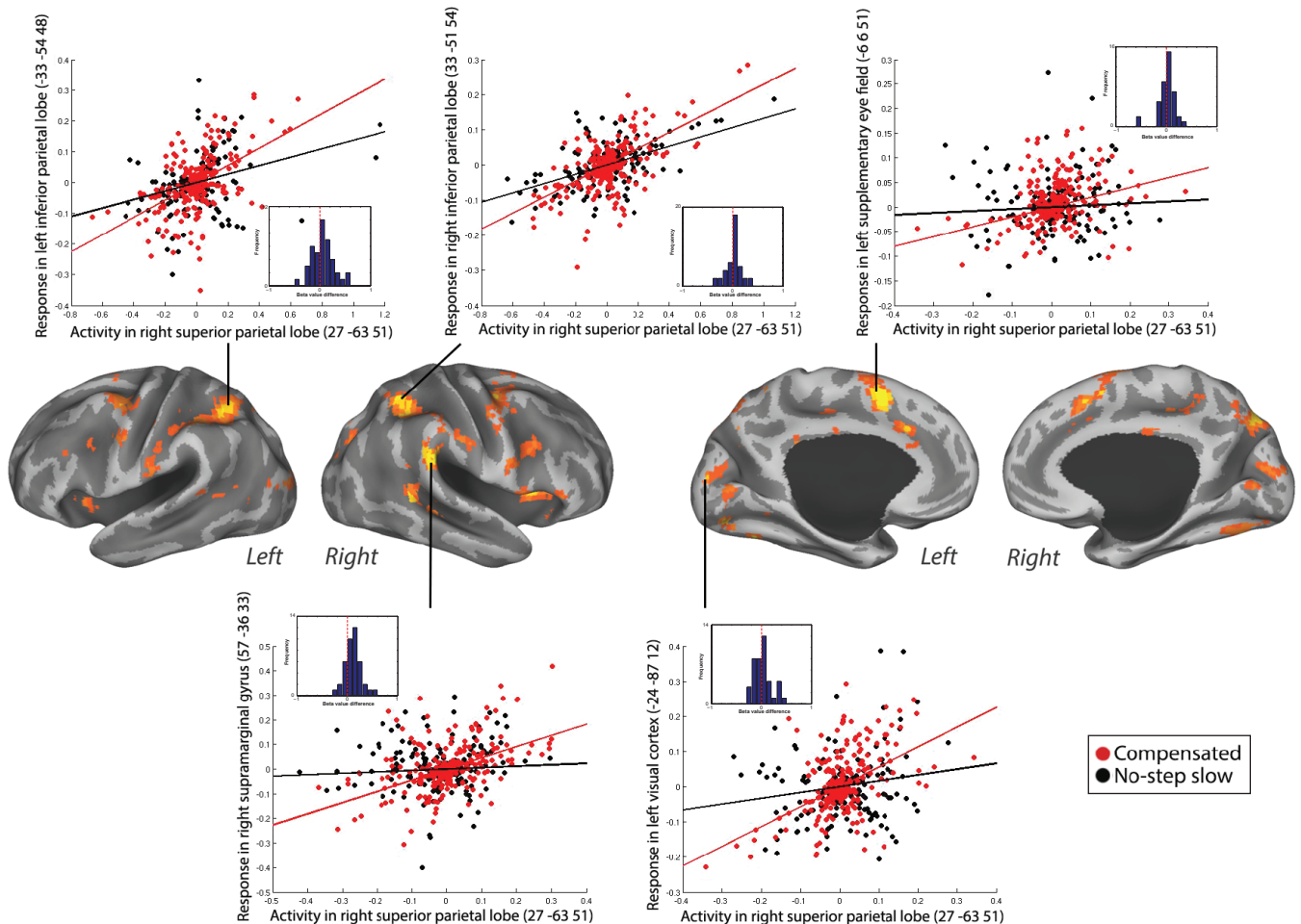


**Figure 4.** Positive PPI between the right SPL (seed) and the response regions, bilateral IPL, left SEF, left visual cortex, and right SMG, for compensated trials versus no-step slow trials in a representative individual. The plots represent the regression of the time series of the seed region (right SPL) on the time series of the responding region. The lines illustrate the regression (red line, compensated trials; black line, no-step slow trials). The dots are the observed data (residual values) adjusted for main effects (red dots, compensated trials; black dots, no-step slow trials). The dots are the residual fMRI time series data (activation factored out) for every single time point in the recorded fMRI time series. For each participant, the slope of line plotting residual activity in the seed against residual activity in the response region was calculated for compensated and no-step slow trials. The difference in the slopes is plotted in the histograms presented in the inset. Positive values represent larger slopes for compensated than no-step slow trials. This was done in order to visualize the data across subjects.

for conflict and error during compensated trials in which there was a chance to make an error.<sup>8,59</sup> IFC activity was also found to be increased for compensated trials. Previous studies on IFC function have shown a role of IFC in saccade inhibition either directly via basal ganglia connections or indirectly by directing the attention to a stop signal.<sup>60,61</sup> These results are also discussed in our previous publication<sup>26</sup> and show for the first time in humans a cortical network that is involved in rapid inhibition and redirection of saccades.

The results of the PPI analyses showed an increased coupling between SPL and other regions of the oculomotor system during compensated trials versus latency-matched no-step trials. More specifically, right SPL showed stronger coupling with frontal oculomotor areas, namely bilateral SEF and right FEF for compensated trials. Based on previous detailed nonhuman primate literature, this increased connectivity

may provide an indirect evidence of SEF-modulating movement activity in FEF neurons via signals from the SPL.<sup>14,15,18</sup> That is, SPL possibly signals to the SEF that targets location, and thus, behavioral demands have changed. The SEF, in turn, could bias the oculomotor system toward a more inhibitory state. This finding of effective connectivity between SPL and FEF and SEF is supported by the findings of anatomical connectivity between the SPL and these frontal oculomotor areas via the superior longitudinal fascicle.<sup>62</sup>

Posterior parts of the brain, including IPL and visual cortex, also showed an increased coupling with right SPL for compensated trials compared to no-step trials. Previous studies have shown that parietal and frontal areas can have a modulatory influence on early visual cortex to guide visual attention.<sup>41,63–66</sup> Our results seem to support these findings. We must note, however, that the direction of these signals

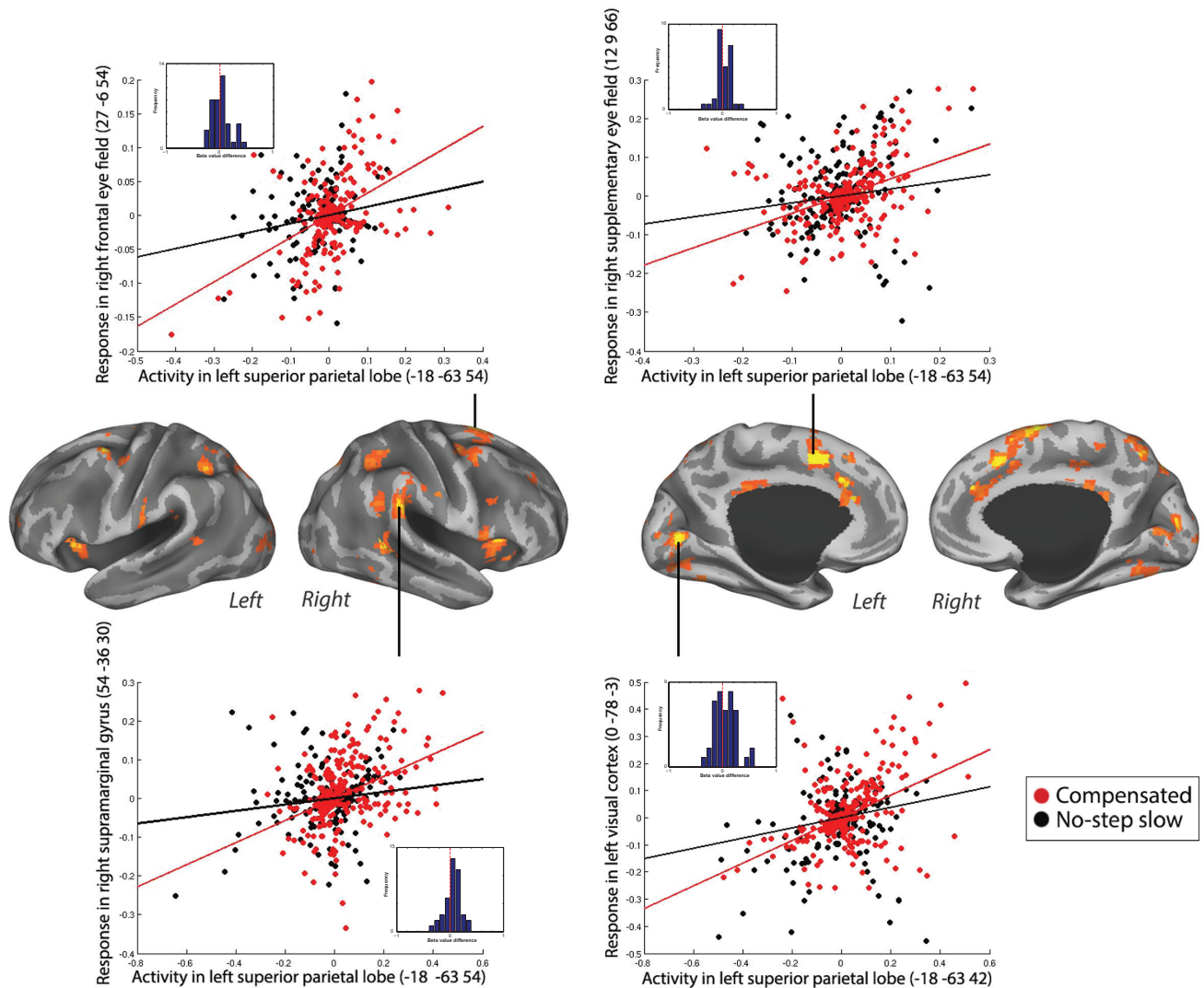


**Figure 5.** Positive PPI between the left SPL (seed) and the response regions, right FEF, right SEF, right SMG, and left visual cortex, for compensated trials versus no-step slow trials in a representative individual. The compensated trials are in red, and the no-step slow trials are in black. The plots represent the regression of the time series of the seed region (left SPL) on the time series of the responding region. The lines illustrate the regression (red line, compensated trials; black line, no-step slow trials). The dots are the observed data (residual values) adjusted for main effects (red dots, compensated trials; black dots, no-step slow trials). The dots are the residual fMRI time series data (activation factored out) for every single time point in the recorded fMRI time series. For each participant, the slope of line plotting residual activity in the seed against residual activity in the response region was calculated for compensated and no-step slow trials. The difference in the slopes is plotted in the histograms presented in the inset. Positive values represent larger slopes for compensated than no-step slow trials. This was done in order to visualize the data across subjects.

cannot be determined using PPI. Thus, it is possible that early visual cortex is modulating SPL instead. Nevertheless, numerous studies have shown that the likely direction of modulation of visual attention is downstream from parietal regions to visual cortex. Attentional processes could also explain the increased coupling between SPL and IPL. IPL is suggested to form an attentional priority map that guides saccadic eye movements.<sup>35–38</sup> Changes in attentional weights in this map are hypothesized to be implemented by the SPL.<sup>36</sup> Increased connectivity between SPL and IPL during compensated trials could reflect this implementation of changes in attentional weights in the priority map. Alternatively, the increased coupling could reflect a process of rapid updating of saccade goal

on compensated trials. IPL function has been associated with spatial orienting while SPL functioning has been related to spatial attention shifts.<sup>35,67–70</sup> After a planned saccade to the first target, an eye-centered reference frame is used to code for target location in FEF and SC. On the appearance of the second target, SPL needs to be updated to compute the motor command of the second eye movement.<sup>31–34</sup> The increased SPL–IPL coupling on compensated trials might reflect an inhibitory process in which orienting to T1 in IPL is inhibited by SPL, thereby allowing the SPL to reorient to T2. Future studies should try to elucidate which explanation is correct.

Subcortically, we observed increased coupling between right SPL and left putamen during compensated trials

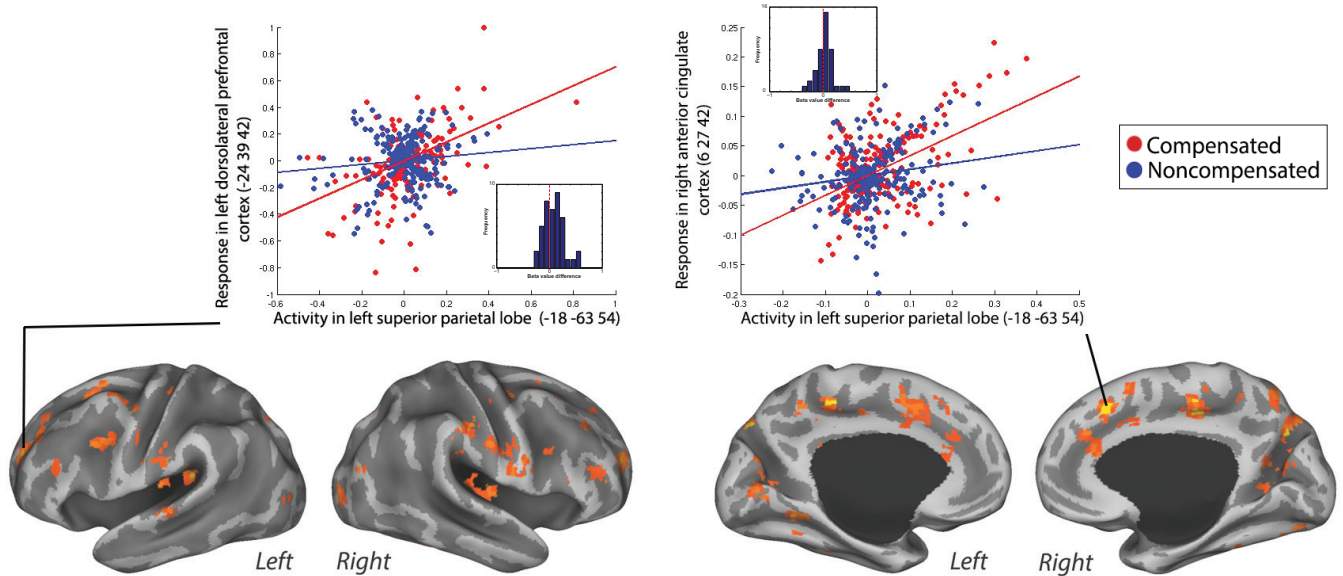


**Figure 6.** Positive PPI between the left SPL (seed) and the response regions left DLPFC and right ACC for compensated trials versus no-step slow trials in a representative individual. The compensated trials are in red, and the noncompensated trials are in blue. The plots represent the regression of the time series of the seed region (left SPL) on the time series of the responding region. The lines illustrate the regression (red line, compensated trials; blue line, noncompensated trials). The dots are the observed data (residual values) adjusted for main effects (red dots, compensated trials; blue dots, noncompensated trials). The dots are residual fMRI time series data (activation factored out) for every single time point in the recorded fMRI time series. For each participant, the slope of line plotting residual activity in the seed against residual activity in the response region was calculated for compensated and noncompensated trials. The difference in the slopes is plotted in the histogram presented in the inset. Positive values represent larger slopes for compensated than noncompensated trials. This was done in order to visualize the data across subjects.

compared to latency-matched no-step trials. Previous literature, mainly from nonhuman primate studies, suggested that the caudate nucleus is involved in saccadic control, while the putamen is strictly involved in skeletomotor control.<sup>26,71,72</sup> However, recent neurophysiology studies and fMRI studies suggested that the putamen is also involved in saccade generation and/or control.<sup>73–77</sup> This new light on the putamen as a saccade control region seems to be supported by our findings since the putamen was more strongly coupled with SPL during inhibition and redirection compared to simple visually guided saccades.

Interestingly, a similar effective connectivity profile in the right hemisphere was found for compensated trials versus no-step trials when left SPL was taken as a seed region (eg, right FEF, right SEF, and right SMG). This interhemispheric coupling might be established by the increased coupling between left SPL and right SPL during compensated trials.<sup>78</sup> Right SPL in turn might signal to right FEF, right SEF, and right SMG to inhibit and redirect the saccades. This right-lateralized network is consistent with previous literature suggesting a right lateralization of the saccadic attentional system.<sup>79–81</sup> Similarly, both activation and connectivity profiles in this study are largely right lateralized.

Successful inhibition compared to unsuccessful inhibition (ie, compensated trials versus noncompensated trials) revealed an increased connectivity with ACC and left DLPFC when left SPL was taken as a seed region. The DLPFC is

involved in the inhibition of saccades.<sup>82</sup> Moreover, it has been suggested that DLPFC neurons integrate signals about task cues and stimulus location to bias the oculomotor system to a more excitatory or inhibitory state, depending on the current task demands.<sup>22</sup> A stronger coupling with the DLPFC could reflect a signal from the SPL of changes in target location. Possibly, these signals are integrated by the DLPFC to inhibit the first planned saccade and initiate a saccade to the new target location.<sup>3</sup> The weaker coupling on noncompensated trials than on compensated trials may reflect the failure to implement the change in spatial attention or target location, resulting in unsuccessful inhibition. On the other hand, stronger SPL–DLPFC coupling on compensated trials versus noncompensated trials might also be related to working memory.<sup>83</sup> Correct task performances rely on task demands being maintained in working memory. Increased coupling might reflect goal information held in working memory that is being used to guide saccadic eye movements. In contrast, a weaker coupling might reflect a failure to use the working memory to guide saccades, which results in unsuccessful inhibition.

Our results also showed an increased coupling between left SPL and ACC during compensated trials as opposed to noncompensated trials. The role of the ACC in saccadic control is debatable. Nonhuman primate studies show that ACC neurons are modulated during errors and reinforcement.<sup>20,21</sup> Human studies, however, suggest that ACC is involved in monitoring the conflict between mutually incompatible





response plans.<sup>84–86</sup> Increased coupling between SPL and ACC might reflect increased signaling of conflict and the need to inhibit planned saccades on redirect trials. A possible mechanism by which inhibition and redirection are implemented on conflicting trials is via early attentional process. That is, fast perceptual detection of the target jump by the SPL might result in rapid inhibition of the saccade by frontal areas due to increased coupling between these areas. Again, we should be careful in interpreting the results from this contrast (ie, compensated versus noncompensated) since putative differences might result from differences in the number of saccades made in each condition (ie, two saccades versus one saccade). However, the visual cortex did not show increased coupling during this PPI analysis. Moreover, the regions that show increased coupling are not specifically labeled as oculomotor areas. This might provide evidence that the differences in the number of eye movements potentially did not influence the results, possibly due to a corrective saccades generated after an error on noncompensated trials.<sup>46</sup> Another point of consideration is that our GLM analysis did not show any area of activation for compensated trials versus noncompensated trials, but we did find changes in coupling for the same contrast. This is not necessarily odd, since PPI and GLM analysis are based on different statistics. The connectivity measure is based on the pattern in residual noise, and how that corresponds between areas, whereas activation maps show to the extent to which average BOLD response amplitudes differ between two conditions. In principle, these metrics are orthogonal in the BOLD data space, so mathematically it is very well possible that there is an activation in a region without connectivity or vice versa. Therefore, theoretically, it is very well possible for a region to be evenly active in both conditions but show a stronger connectivity (ie, interaction) with the seed region in one condition over another. Finally, findings from the PPI analysis in which we compared connectivity during compensated trials with noncompensated trials do not resemble findings from the PPI analysis in which connectivity on compensated trials was compared to no-step trials. However, it is important to note that in the first contrast (ie, compensated versus noncompensated), a certain amount of *cognitive control* was assumed to be implemented by the participant in both conditions, but this cognitive control did not *win* on noncompensated trials. Differences in this contrast, therefore, reflect the success of implementing cognitive control rather than reflecting the process of implementing cognitive control per se.

Consistent with previous studies,<sup>35–38</sup> our findings suggest a role of SPL in rapid control over saccadic eye movements, potentially via early attentional processes. The importance of early sensory and attentional processes in rapid inhibition and redirection of planned movements has been addressed in recent computational modeling studies.<sup>45,86</sup> During countermanding task performance, afferent processing time of the signal to stop/change a response makes up the bulk of stop signal reaction time, the estimated latency

to inhibit a planned action. Several experimental studies have also shown that stop signal reaction time is related to the sensory discrimination of relevant signals.<sup>44,87,88</sup> In the context of the race model of countermanding task performance, whereby successful inhibition is based on a race between GO and STOP processes that begin upon presentation of the signal to initiate and inhibit movement, respectively,<sup>49,50</sup> faster perceptual processing causes faster initiation of the STOP process. This increases the likelihood that the STOP signal finishes first. As a consequence, the initial planned saccade is inhibited. Alternatively, rapid updating of saccade goal is also relevant during rapid control of saccades. The desired endpoint needs to be encoded in a spatial reference frame allowing fast saccadic reprogramming and associated spatial updating across saccades, a capacity related to SPL functioning.<sup>31,34</sup> Our results, together with previous studies, provide new evidence that SPL might be an important area in higher order control over saccades embedded in the oculomotor network.

A limitation of this study is that with PPI analysis it is impossible to draw conclusions on the precise pathway via which SPL influences other oculomotor areas.<sup>56</sup> PPI measures the correlation between time series in a seed region and another region during a specific task condition. This does not necessarily imply that those areas are anatomically connected. This correlation could also act via the third structure or this third structure could exert a condition-specific modulation on the activity in the seed and the response region. Therefore, we should be careful about drawing firm conclusions about the underlying pathways. However, human dissection studies and noninvasive techniques, such as diffusion tensor imaging, could add to our understanding of the underlying anatomical pathway of these functional networks.<sup>62,89–91</sup> A related limitation of PPI analysis is that we cannot infer on the directionality because PPI measures task-related differences in a correlation between activation in two regions. That does not mean that the seed region is the causative agent of this correlated activity. A possible direction for future studies is to use dynamic causal modeling. Dynamic causal modeling enables us to test the architecture of different neural models and the causality of neural activity in a context-dependent manner.<sup>92</sup> This would allow for firm conclusions on the underlying pathway and directionality of activity.

This study emphasizes the importance of taking SPL into account when studying the neural circuitry of executive control. This can especially have important implications for studying the neural basis of abnormal reactive control of saccades seen in neuropsychiatric disorders, such as schizophrenia,<sup>93</sup> ADHD,<sup>44,94</sup> and Parkinson's disease,<sup>95</sup> as these impairments might have their basis in early sensory and attentional processes, rather than inhibition per se.

## Conclusion

To conclude, in this study, we observed changes in effective connectivity between the SPL and other oculomotor areas





(eg, FEF, SEF, and visual cortex) that contributed significantly to the rapid control over eye movements, potentially via early attention control or rapid updating of saccade goal. This network of frontal and posterior areas enables us to rapidly inhibit and change plans. Our findings have implications for understanding the mechanism that enables us to rapidly control our behavior and how action control is affected in neuropsychiatric disorders.

### Acknowledgments

We thank Dr Jeffrey Schall, Dr Bram Zandbelt, and Dr Stefan van der Stigchel for their contributions to the experimental design. We thank Fiona van der Heiligenberg, Helene Hopman, and Ilse Anne Thompson for their contributions to collecting and analyzing the data.

### Author Contributions

Conceived and designed the experiments: KNT and SFWN. Analyzed the data: SJA and KNT. Wrote the first draft of the article: SJA. Contributed to the writing of the article: SJA, KNT, and SFWN. Agreed the study results and conclusions: SJA, KNT, and SFWN. Jointly developed the structure and arguments for the article: SJA, KNT, and SFWN. Made the critical revisions and approved the final version: SJA, KNT, and SFWN. All authors reviewed and approved the final article.

### REFERENCES

- Aron AR. From reactive to proactive and selective control: developing a richer model for stopping inappropriate responses. *Biol Psychiatry*. 2011;69(12):e55–e68.
- Schall JD. Neural basis of deciding, choosing and acting. *Nat Rev Neurosci*. 2001; 2(1):33–42.
- Munoz DP, Everling S. Look away: the anti-saccade task and the voluntary control of eye movement. *Nat Rev Neurosci*. 2004;5(3):218–228.
- Hutton SB. Cognitive control of saccadic eye movements. *Brain Cogn*. 2008;68(3): 327–340.
- Leigh RJ, Kennard C. Using saccades as a research tool in the clinical neurosciences. *Brain*. 2004;127(pt 3):460–477.
- Hikosaka O, Takikawa Y, Kawagoe R. Role of the basal ganglia in the control of purposive saccadic eye movements. *Physiol Rev*. 2000;80(3):953–979.
- Munoz DE. Commentary: saccadic eye movements: overview of neural circuitry monkey. *Prog Brain Res*. 2002;140:89–96.
- Schall JD, Boucher L. Executive control of gaze by the frontal lobes. *Cogn Affect Behav Neurosci*. 2007;7(4):396–412.
- Camalier CR, Gotler A, Murthy A, et al. Dynamics of saccade target selection: race model analysis of double step and search step saccade production in human and macaque. *Vision Res*. 2007;47(16):2187–2211.
- Murthy A, Ray S, Shorter SM, Schall JD, Thompson KG. Neural control of visual search by frontal eye field: effects of unexpected target displacement on visual selection and saccade preparation. *J Neurophysiol*. 2009;101(5):2485–2506.
- Ramakrishnan A, Sureshbabu R, Murthy A. Understanding how the brain changes its mind: microstimulation in the macaque frontal eye field reveals how saccade plans are changed. *J Neurosci*. 2012;32(13):4457–4472.
- Bruce CJ, Goldberg ME. Primate frontal eye fields. I. Single neurons discharging before saccades. *J Neurophysiol*. 1985;53(3):603–635.
- Everling S, Munoz DP. Neuronal correlates for preparatory set associated with pro-saccades and anti-saccades in the primate frontal eye field. *J Neurosci*. 2000;20(1):387–400.
- Hanes DP, Schall JD. Neural control of voluntary movement initiation. *Science*. 1996;274(5286):427–430.
- Hanes DP, Patterson WF, Schall JD. Role of frontal eye fields in countermanding saccades: visual, movement, and fixation activity. *J Neurophysiol*. 1998;79(2): 817–834.
- Pouget P, Emeric EE, Stuphorn V, Reis K, Schall JD. Chronometry of visual responses in frontal eye field, supplementary eye field, and anterior cingulate cortex. *J Neurophysiol*. 2005;94(3):2086–2092.
- Stuphorn V, Taylor TL, Schall JD. Performance monitoring by the supplementary eye field. *Nature*. 2000;408(6814):857–860.
- Stuphorn V, Schall JD. Executive control of countermanding saccades by the supplementary eye field. *Nat Neurosci*. 2006;9(7):925–931.
- Stuphorn V, Brown JW, Schall JD. Role of supplementary eye field in saccade initiation: executive, not direct, control. *J Neurophysiol*. 2010;103(2):801–816.
- Ito S, Stuphorn V, Brown JW, Schall JD. Performance monitoring by the anterior cingulate cortex during saccade countermanding. *Science*. 2003;302(5642): 120–122.
- Emeric EE, Brown JW, Leslie M, Pouget P, Stuphorn V, Schall JD. Performance monitoring local field potentials in the medial frontal cortex of primates: anterior cingulate cortex. *J Neurophysiol*. 2008;99(2):759–772.
- Funahashi S, Chafee MV, Goldman-Rakic PS. Prefrontal neuronal activity in rhesus monkeys performing a delayed anti-saccade task. *Nature*. 1993;365(6448): 753–756.
- Wurtz RH, Albano JE. Visual-motor function of the primate superior colliculus. *Annu Rev Neurosci*. 1980;3:189–226.
- Connolly JD, Goodale MA, Goltz HC, Munoz DP. fMRI activation in the human frontal eye field is correlated with saccadic reaction time. *J Neurophysiol*. 2005;94(1):605–611.
- Schall JD, Stuphorn V, Brown JW. Monitoring and control of action by the frontal lobes. *Neuron*. 2002;36(2):309–322.
- Thakkar KN, van den Heiligenberg FMZ, Kahn RS, Neggers SFW. Frontal-subcortical circuits involved in reactive control and monitoring of gaze. *J Neurosci*. 2014;34(26):8918–8929.
- Rizzolatti G, Matelli M. Two different streams form the dorsal visual system: anatomy and functions. *Exp Brain Res*. 2003;153(2):146–157.
- Sereno MI, Pitzalis S, Martinez A. Mapping of contralateral space in retinotopic coordinates by a parietal cortical area in humans. *Science*. 2001;294(5545): 1350–1354.
- Grefkes C, Fink GR. The functional organization of the intraparietal sulcus in humans and monkeys. *J Anat*. 2005;207(1):3–17.
- Wardak C, Olivier E, Duhamel J-R. Saccadic target selection deficits after lateral intraparietal area inactivation in monkeys. *J Neurosci*. 2002;22(22):9877–9884.
- Andersen R, Bracewell R, Barash S, Gnadt J, Fogassi L. Eye position effects on visual, memory, and saccade-related activity in areas LIP and 7a of macaque. *J Neurosci*. 1990;10(4):1176–1196.
- Brotchie PR, Andersen RA, Snyder LH, Goodman SJ. Head position signals used by parietal neurons to encode locations of visual stimuli. *Nature*. 1995; 375(6528):232–235.
- Snyder L, Batista A, Andersen R. Coding of intention in the posterior parietal cortex. *Nature*. 1997;386:167–170.
- Medendorp WP, Goltz HC, Vilis T, Crawford JD. Gaze-centered updating of visual space in human parietal cortex. *J Neurosci*. 2003;23(15):6209–6214.
- Vandenberghe R, Gitelman DR, Parrish TB, Mesulam MM. Functional specificity of superior parietal mediation of spatial shifting. *Neuroimage*. 2001;14(3): 661–673.
- Molenberghs P, Mesulam MM, Peeters R, Vandenberghe RRC. Remapping attentional priorities: differential contribution of superior parietal lobule and intraparietal sulcus. *Cereb Cortex*. 2007;17(11):2703–2712.
- Serences JT, Yantis S. Spatially selective representations of voluntary and stimulus-driven attentional priority in human occipital, parietal, and frontal cortex. *Cereb Cortex*. 2007;17(2):284–293.
- Yantis S, Schwarzbach J, Serences JT, et al. Transient neural activity in human parietal cortex during spatial attention shifts. *Nat Neurosci*. 2002;5(10):995–1002.
- Shomstein S, Lee J, Behrmann M. Top-down and bottom-up attentional guidance: investigating the role of the dorsal and ventral parietal cortices. *Exp Brain Res*. 2010;206(2):197–208.
- Verfaellie M, Rapcsak SZ, Heilman KM. Impaired shifting of attention in Balint's syndrome. *Brain Cogn*. 1990;12(2):195–204.
- Van Ettinger-Veenstra HM, Huijbers W, Gutteling TP, Vink M, Kenemans JL, Neggers SFW. fMRI-guided TMS on cortical eye fields: the frontal but not intraparietal eye fields regulate the coupling between visuospatial attention and eye movements. *J Neurophysiol*. 2009;102(6):3469–3480.
- Matsuda T, Matsuura M, Ohkubo T, et al. Functional MRI mapping of brain activation during visually guided saccades and antisaccades: cortical and subcortical networks. *Psychiatry Res*. 2004;131(2):147–155.
- Kimmig H, Greenlee MW, Gondan M, Schira M, Kassubek J, Mergner T. Relationship between saccadic eye movements and cortical activity as measured by fMRI: quantitative and qualitative aspects. *Exp Brain Res*. 2001;141(2):184–194.
- Armstrong IT, Munoz DP. Inhibitory control of eye movements during oculomotor countermanding in adults with attention-deficit hyperactivity disorder. *Exp Brain Res*. 2003;152(4):444–452.
- Salinas E, Stanford TR. The countermanding task revisited: fast stimulus detection is a key determinant of psychophysical performance. *J Neurosci*. 2013;33(13): 5668–5685.



46. Murthy A, Ray S, Shorter SM, Priddy EG, Schall JD, Thompson KG. Frontal eye field contributions to rapid corrective saccades. *J Neurophysiol.* 2007;97(2):1457–1469.
47. Van der Stigchel S, Nijboer TC. The global effect: what determines where the eyes land? *J Eye Mov Res.* 2011;4(2):1–13.
48. Ashburner J, Barnes G, Chen C, et al. *SPM8 Manual*. Functional Imaging Laboratory Wellcome Trust Centre for Neuroimaging Institute of Neurology, London, UK, 2011.
49. Logan GD, Cowan WB. On the ability to inhibit thought and action: a theory of an act of control. *Psychol Rev.* 1984;91(3):295–327.
50. Verbruggen F, Logan GD. Models of response inhibition in the stop-signal and stop-change paradigms. *Neurosci Biobehav Rev.* 2009;33(5):647–661.
51. Glover GH, Li TQ, Ress D. Image-based method for retrospective correction of physiological motion effects in fMRI: RETROICOR. *Magn Reson Med.* 2000;44(1):162–167.
52. Behzadi Y, Restom K, Liu J, Liu TT. A component based noise correction method (CompCor) for BOLD and perfusion based fMRI. *Neuroimage.* 2007;37(1):90–101.
53. Van Dijk KRA, Hedden T, Venkataraman A, Evans KC, Lazar SW, Buckner RL. Intrinsic functional connectivity as a tool for human connectomics: theory, properties, and optimization. *J Neurophysiol.* 2010;103(1):297–321.
54. Worsley K, Evans A. A three-dimensional statistical analysis for CBF activation studies in human brain. *Cereb Blood Flow.* 1992;12:900.
55. Worsley K, Marrett S, Neelin P. A unified statistical approach for determining significant signals in images of cerebral activation. *Hum Brain Mapp.* 1996;4(1):58–73.
56. Friston KJ, Buechel C, Fink GR, Morris J, Rolls E, Dolan RJ. Psychophysiological and modulatory interactions in neuroimaging. *Neuroimage.* 1997;6(3):218–229.
57. Tzourio-Mazoyer N, Landeau B, Papathanassiou D, et al. Automated anatomical labeling of activations in SPM using a macroscopic anatomical parcellation of the MNI MRI single-subject brain. *Neuroimage.* 2002;15(1):273–289.
58. Curtis CE, Cole MW, Rao VY, D'Esposito M. Canceling planned action: an fMRI study of countermanding saccades. *Cereb Cortex.* 2004;15(9):1281–1289.
59. Sharika KM, Neggess SFW, Gutteling TP, Van der Stigchel S, Dijkerman HC, Murthy A. Proactive control of sequential saccades in the human supplementary eye field. *Proc Natl Acad Sci U S A.* 2013;110(14):E1311–E1320.
60. Nambu A, Tokuno H, Takada M. Functional significance of the cortico-subthalamic-pallidal “hyperdirect” pathway. *Neurosci Res.* 2002;43(2):111–117.
61. Sharp DJ, Bonnelle V, De Boissezon X, et al. Distinct frontal systems for response inhibition, attentional capture, and error processing. *Proc Natl Acad Sci U S A.* 2010;107(13):6106–6111.
62. Makris N, Kennedy DN, McInerney S, et al. Segmentation of subcomponents within the superior longitudinal fascicle in humans: a quantitative, in vivo, DT-MRI study. *Cereb Cortex.* 2005;15(6):854–869.
63. Kastner S, Pinsk MA, De Weerd P, Desimone R, Ungerleider LG. Increased activity in human visual cortex during directed attention in the absence of visual stimulation. *Neuron.* 1999;22(4):751–761.
64. Bressler SL, Tang W, Sylvester CM, Shulman GL, Corbetta M. Top-down control of human visual cortex by frontal and parietal cortex in anticipatory visual spatial attention. *J Neurosci.* 2008;28(40):10056–10061.
65. Gutteling TP, van Ettinger-Veenstra HM, Kenemans JL, Neggess SFW. Lateralized frontal eye field activity precedes occipital activity shortly before saccades: evidence for cortico-cortical feedback as a mechanism underlying covert attention shifts. *J Cogn Neurosci.* 2010;22(9):1931–1943.
66. Neggess SFW, Huijbers W, Vrijlandt CM, Vlaskamp BNS, Schutter DJLG, Kenemans JL. TMS pulses on the frontal eye fields break coupling between visuospatial attention and eye movements. *J Neurophysiol.* 2007;98(5):2765–2778.
67. Ciavarrò M, Ambrosini E, Tosoni A, Committeri G, Fattori P, Galletti C. rTMS of medial parieto-occipital cortex interferes with attentional reorienting during attention and reaching tasks. *J Cogn Neurosci.* 2013;25(9):1453–1462.
68. Corbetta M. Frontoparietal cortical networks for directing attention and the eye to visual locations: identical, independent, or overlapping neural systems? *Proc Natl Acad Sci U S A.* 1998;95(3):831–838.
69. Shomstein S. Cognitive functions of the posterior parietal cortex: top-down and bottom-up attentional control. *Front Integr Neurosci.* 2012;6:38.
70. Hopfinger JB, Buonocore MH, Mangun GR. The neural mechanisms of top-down attentional control. *Nat Neurosci.* 2000;3(3):284–291.
71. Cameron IGM, Coe BC, Watanabe M, Stroman PW, Munoz DP. Role of the basal ganglia in switching a planned response. *Eur J Neurosci.* 2009;29(12):2413–2425.
72. Watanabe M, Munoz DP. Presetting basal ganglia for volitional actions. *J Neurosci.* 2010;30(30):10144–10157.
73. Ford KA, Gati JS, Menon RS, Everling S. BOLD fMRI activation for anti-saccades in nonhuman primates. *Neuroimage.* 2009;45(2):470–476.
74. Phillips JM, Everling S. Neural activity in the macaque putamen associated with saccades and behavioral outcome. *PLoS One.* 2012;7(12):e51596.
75. Aichert DS, Williams SCR, Möller H-J, Kumari V, Ettinger U. Functional neural correlates of psychometric schizotypy: an fMRI study of antisaccades. *Psychophysiology.* 2012;49(3):345–356.
76. Neggess SFW, Diepen RM, Zandbelt BB, Vink M, Mandl RCW, Gutteling TP. A functional and structural investigation of the human fronto-basal volitional saccade network. *PLoS One.* 2012;7(1):e29517.
77. Neggess SFW, Zandbelt BB, Schall MS, Schall JD. Comparative diffusion tractography of corticostriatal motor pathways reveals differences between humans and macaques. *J Neurophysiol.* 2015;113(7):2164–2172.
78. Jarbo K, Verstynen T, Schneider W. In vivo quantification of global connectivity in the human corpus callosum. *Neuroimage.* 2012;59(3):1988–1996.
79. Thiebaut de Schotten M, Dell'Acqua F, Forkel SJ, et al. A lateralized brain network for visuospatial attention. *Nat Neurosci.* 2011;14(10):1245–1246.
80. Petit L, Zago L, Vigneau M, et al. Functional asymmetries revealed in visually guided saccades: an fMRI study. *J Neurophysiol.* 2009;102(5):2994–3003.
81. Corbetta M, Shulman GL. Control of goal-directed and stimulus-driven attention in the brain. *Nat Rev Neurosci.* 2002;3(3):201–215.
82. Hasegawa RP, Peterson BW, Goldberg ME. Prefrontal neurons coding suppression of specific saccades. *Neuron.* 2004;43(3):415–425.
83. Owen AM, Evans AC, Petrides M. Evidence for a two-stage model of spatial working memory processing within the lateral frontal cortex: a positron emission tomography study. *Cereb Cortex.* 1996;6(1):31–38.
84. Botvinick MM, Braver TS, Barch DM, Carter CS, Cohen JD. Conflict monitoring and cognitive control. *Psychol Rev.* 2001;108(3):624–652.
85. Botvinick M, Braver T. Evaluating the demand for control: Anterior cingulate cortex and conflict monitoring. Technical Report 98.1, Center for the Neural Basis of Cognition, Pittsburgh, Pennsylvania, 1998.
86. Boucher L, Palmeri TJ, Logan GD, Schall JD. Inhibitory control in mind and brain: an interactive race model of countermanding saccades. *Psychol Rev.* 2007;114(2):376–397.
87. Stanford TR, Shankar S, Massoglia DP, Costello MG, Salinas E. Perceptual decision making in less than 30 milliseconds. *Nat Neurosci.* 2010;13(3):379–385.
88. Shankar S, Massoglia DP, Zhu D, Costello MG, Stanford TR, Salinas E. Tracking the temporal evolution of a perceptual judgment using a compelled-response task. *J Neurosci.* 2011;31(23):8406–8421.
89. Catani M, Howard RJ, Pajevic S, Jones DK. Virtual in vivo interactive dissection of white matter fasciculi in the human brain. *Neuroimage.* 2002;17(1):77–94.
90. Thiebaut de Schotten M, Dell'Acqua F, Valabregue R, Catani M. Monkey to human comparative anatomy of the frontal lobe association tracts. *Cortex.* 2012;48(1):82–96.
91. Martino J, De Witt Hamer PC, Berger MS, et al. Analysis of the subcomponents and cortical terminations of the perisylvian superior longitudinal fasciculus: a fiber dissection and DTI tractography study. *Brain Struct Funct.* 2013;218(1):105–121.
92. Friston KJ, Harrison L, Penny W. Dynamic causal modelling. *Neuroimage.* 2003;19(4):1273–1302.
93. Thakkar KN, Schall JD, Boucher L, Logan GD, Park S. Response inhibition and response monitoring in a saccadic countermanding task in schizophrenia. *Biol Psychiatry.* 2011;69(1):55–62.
94. Hanisch C, Radach R, Holtkamp K, Herpertz-Dahlmann B, Konrad K. Oculomotor inhibition in children with and without attention-deficit hyperactivity disorder (ADHD). *J Neural Transm.* 2006;113(5):671–684.
95. Joti P, Kulashakar S, Behari M, Murthy A. Impaired inhibitory oculomotor control in patients with Parkinson's disease. *Exp Brain Res.* 2007;177(4):447–457.